Supporting Information

Exploring long-range cooperativity in the 20S proteasome core particle from *T. acidophilum* using methyl-TROSY based NMR spectroscopy

www.pnas.org/cgi/doi/10.1073/pnas.1920770117

Gating cooperativity tested with 11S RP binding

As described in the text, binding of the 11S RP particle to asymmetric CPs (one α_7-ring, M1I+M6A+K66A+S95C, is ILVM-$^{13}CH_3$ labeled and a second ring, M1I+M6A+S95C, is unlabeled) is analyzed using a pair of distinct models that either assume no gating cooperativity between α_7-rings at opposite ends of the barrel or maximum cooperativity. We focus here on the model that assumes maximum cooperativity and describe it in more detail. As the α_7-ring that comprises site II is ILVM labeled, and hence observed in NMR spectra, we consider the gates from this ring exclusively. Our goal is to derive expressions for $p(in)$, $p(out)$, and $p(tet)$ for this site that can be compared with experimental data. To do this we assume that upon 11S RP binding to one of the two α_7-rings of the 20S CP, the gates of the bound α_7-ring assume an *in*, *out*, and *tet* distribution that is given by $p(in|y^{BD})$, $p(out|y^{BD})$, and $p(tet|y^{BD})$, where y^{BD} = I^{BD} or II^{BD}, depending on whether binding occurs at site I or site II, respectively. That is, binding of the 11S RP at one site of the CP leads to the same gating equilibria at that site as for an isolated α_7-ring that is 11S RP bound. Thus, when the 11S RP is bound to site II, irrespective of whether site I is in the bound state or not, $p(in|II^{BD})$, $p(out|II^{BD})$ and $p(tet|II^{BD})$ values are equal to the corresponding p values measured for the isolated M1I+M6A+K66A+S95C α_7-ring (see text). Second, in a configuration in which one site is 11S bound and the second site is not, the populations *in* and *out* gates at the unbound site are shifted to reflect the populations at the bound site, with the gates at the unbound end of the CP slaved to those at the bound site (maximum cooperativity, see below).

Given these two assumptions we are now in a position to calculate p values, noting that there are four different 11S RP bound/unbound configurations, as illustrated in Figure 3c, which we denote as structures 1 - 4. The gating probabilities are described below for each of these four structures:

- In the **1st structure** both sides of the CP are unbound and the probability of an *in* or an *out* gate is simply $p^o(in)$, $p^o(out)$, that has been measured to be 2/7 or 5/7, both for isolated α_7 particles[1-2] and the full 20S CP[1].
- In contrast, in the **4th structure** both sides of the CP are 11S bound. The p values for site II are given by $p(in|II^{BD})$, $p(out|II^{BD})$ and $p(tet|II^{BD})$, as the gating equilibrium is dictated by the fact that this site is 11S RP bound. It is noteworthy that the corresponding $p(in|I^{BD})$, $p(out|I^{BD})$ and $p(tet|I^{BD})$ values are the same as those for site II, to within experimental error (recall that $p(tet|II^{BD})$ was set equal to $p(tet|I^{BD})$, see text), so that the gating distribution of each side is effectively the same irrespective of any cooperativity, as for structure 1.
- Similarly, in the case of **structure 2** the p values for site II are given by $p(in|II^{BD})$, $p(out|II^{BD})$ and $p(tet|II^{BD})$, as site II is bound.
- The notion of cooperativity becomes important in the context of deriving p values for the gates at site II of **structure 3**, where site I is 11S bound and site II is not. As discussed above in this case, and assuming maximum cooperativity, site II becomes slaved to site I so that the shift in site I gates

towards the *out* + *tethered* configurations that accompanies the 11S RP binding translates to a corresponding shift in the gates at site II towards the *out* state. Thus, we can write

$$p(in, 3^{rd}\ structure) = p(\mathrm{I}^{\mathrm{BD}}) \cdot (1 - p(\mathrm{II}^{\mathrm{BD}})) \cdot p(in \mid \mathrm{I}^{\mathrm{BD}})$$
$$p(out, 3^{rd}\ structure) = p(\mathrm{I}^{\mathrm{BD}}) \cdot (1 - p(\mathrm{II}^{\mathrm{BD}})) \cdot (1 - p(in \mid \mathrm{I}^{\mathrm{BD}}))$$

The first two terms in each of the above expressions give the probability of a 20S CP with an 11S RP-bound K66 ring (site I) and an unbound (*i.e.*, no 11S) K66A-ring (site II). The subsequent term in the expression for $p(in)$, $p(in|\mathrm{I}^{\mathrm{BD}})$, is the conditional probability of finding a site I gate in the *in* position given that site I is bound. As site II is assumed to be very strongly coupled to site I, this is the probability of an *in* site II gate as well. Similarly, the $(1- p(in|\mathrm{I}^{\mathrm{BD}}))$ term in the second expression is the probability of finding a site I gate in the *out* or *tethered* position (anything but *in*) when the 11S RP is bound to this site. Again, because site II is slaved to site I, this is also the probability of a site II gate in the *out* position. (Note that a tethered gate position in site I is effectively an *out* position so that tethered gates at site I "push" gates in site II to the *out* state in the 3rd structure).

It is worth noting that the four structures in Figure 3c can be used to calculate expressions for $p(in)$ and $p(out)$ in the limit of no cooperativity. As cooperativity is introduced only for structure 3, the expressions underneath the other three structures are valid in this other limiting case (no cooperativity) as well. If the $p(in|\mathrm{I}^{\mathrm{BD}})$ and $1- p(in|\mathrm{I}^{\mathrm{BD}})$ terms for $p(in)$ and $p(out)$ (structure 3) are replaced by $p^o(in)$ and $p^o(out)$, respectively, as the gating status at one end is no longer affected by the other side in the limit of no allostery, Eq. [1] of the main text is then obtained.

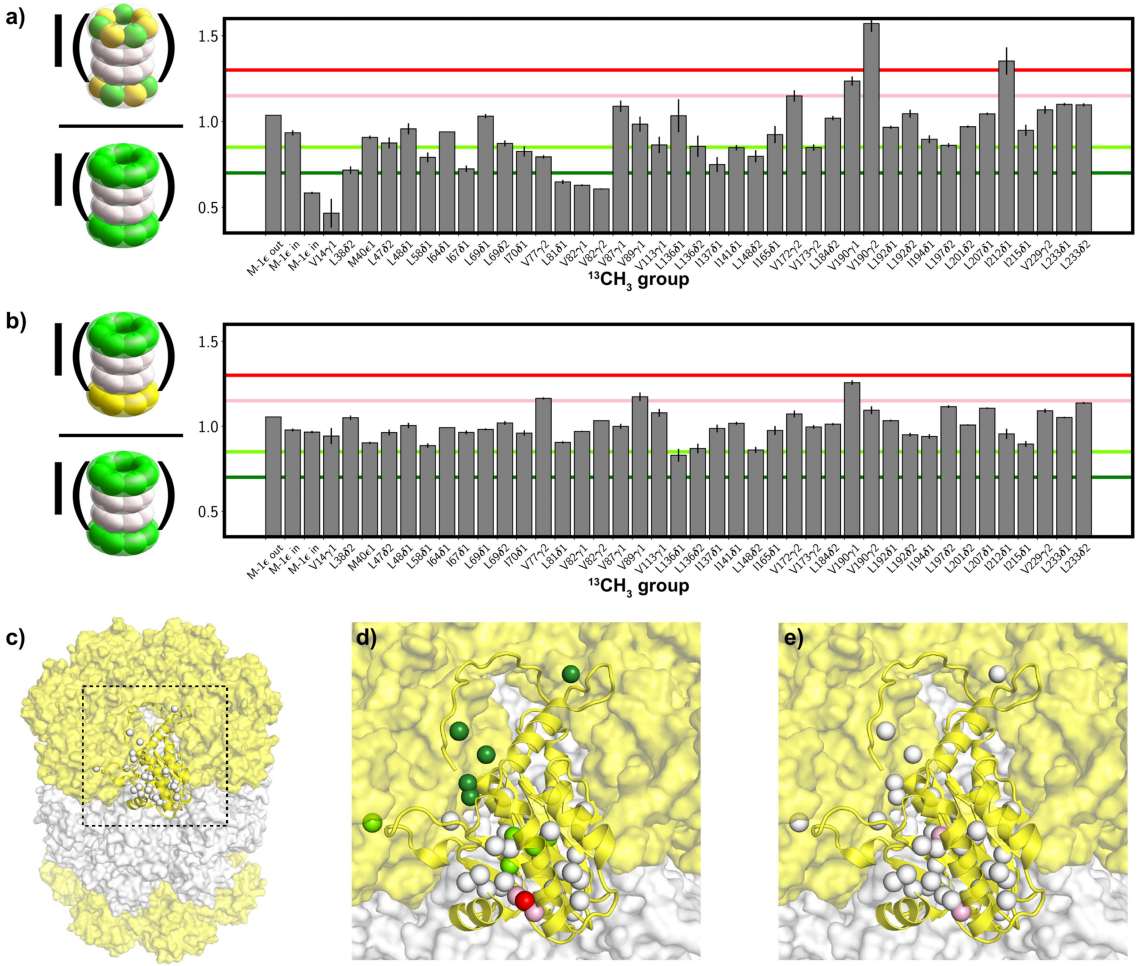

Figure S1. Scrambling of α-subunits is minimal during the generation and purification of asymmetric 20S CPs and subsequent NMR data acquisition. Two types of α-subunits were used, including ILVM-$^{13}CH_3$ labeled M1I+M6A+S95C (green spheres) and natural abundance S95C (yellow spheres) protomers. Three 20S CP samples were produced: (1) a symmetric ILVM-$^{13}CH_3$ labeled M1I+M6A+S95C 20S CP (green α_7-rings); (2) a completely scrambled 20S CP (α_7-rings are comprised of green and yellow subunits) and (3) an asymmetric 20S CP, as described in the text (1 green and 1 yellow α_7-ring). The scrambled sample was obtained by mixing the two different α subunits at an equimolar ratio followed by unfolding in 8M GdnDCl, refolding by fast dilution to generate randomly mixed α_7-rings and finally the CP was generated as before[2]. Unfolding and refolding was done in D_2O solutions using deuterated GdnDCl, to prevent D/H hydrogen exchange of buried exchangeable protons. GdnDCl was prepared by repeated cycles of dissolution of guanidine hydrochloride in heavy water followed by evaporation in a SpeedVac system. ^{13}C-^{1}H HMQC spectra were recorded of each sample and peak intensities (measured with the nmrPipe routine nlinLS[3]) obtained. Peak intensities were scaled appropriately to reflect the different numbers of labeled protomers in samples with 7 of the 14 subunits ILVM-labeled and all 14 subunits labeled. (a,b) Bar plots of intensity ratios, as indicated. Lines delineate ratios of 0.7 (dark green), 0.85 (light green), 1.15 (pink), and 1.3 (red). (c) Full proteasome, highlighting region used for expanded plot in panels (d) and (e). (d,e) Methyl

groups with intensity ratios, r, such that $r < 0.7$, $0.7 < r < 0.85$, $0.85 < r < 1.15$, $1.15 < r < 1.3$, $r > 1.3$ are colored dark green, light green, white, pink, and red, respectively. Ratios for the scrambled (d) and asymmetric (e) samples are indicated. Note how intensity ratios deviate considerably from 1 in the scrambled sample (a,d), especially close to the interface between α protomers, but not for the asymmetric sample (b,e).

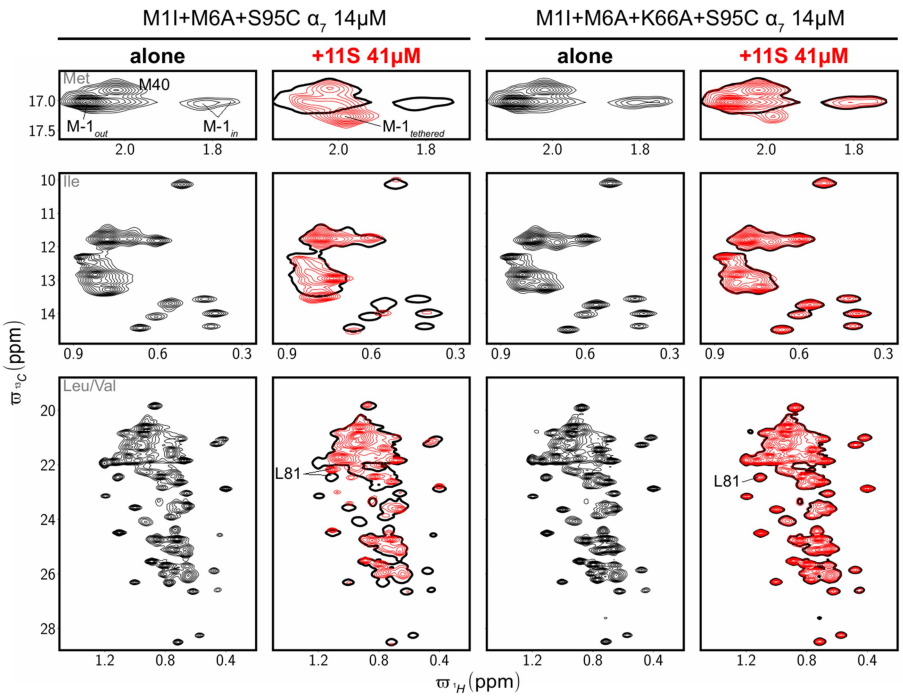

Figure S2. Effect of the K66A mutation on the binding of the 11S RP to isolated α_7-rings. Spectral regions for the two α_7 variants, ILVM-$^{13}CH_3$ labeled M1I+M6A+S95C α_7 (left) and ILVM-$^{13}CH_3$ labeled M1I+M6A+K66A+S95C α_7 (right) are shown with spectra of α_7 alone and in the presence of the 11S RP contoured in black and red, respectively.

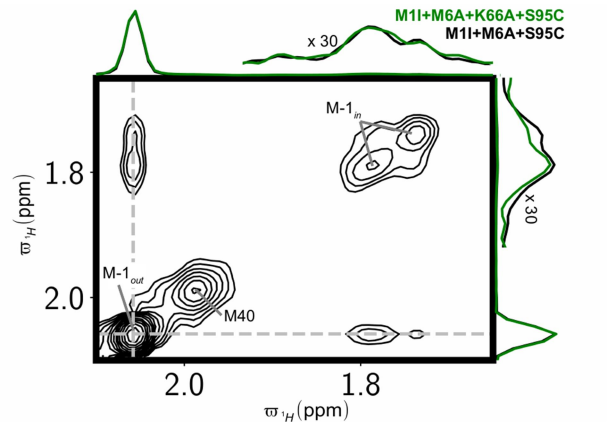

Figure S3. Gating *in*/*out* kinetics are similar for K66 and K66A α_7-rings. Magnetization exchange experiments[1] were recorded with a mixing time of 0.4 s for both K66 (black) and K66A (green) samples, 45°C, 800 MHz, with traces from positions indicated by dashed grey lines shown above and to the side of the main spectrum. Cross-peaks, connecting *M-1*$_{out}$ and *M-1*$_{in}$, derive from an exchange process in which gates interconvert between *in* and *out* states during the mixing time, while diagonal peaks derive from gates residing in the same state during the mixing time. The near superposition of cross peak intensities indicates that the exchange kinetics are similar for both K66 and K66A rings. We have not attempted to record a time-course from which exchange rates could be fit, as the low concentrations (14 μM of α_7-rings) of samples precludes such a quantitative analysis without extensive measurement times. Traces from data sets recorded on K66 and K66A samples were normalized using maximum M-1$_{out}$ diagonal peak intensities from spectra recorded with a mixing time of 0 s.

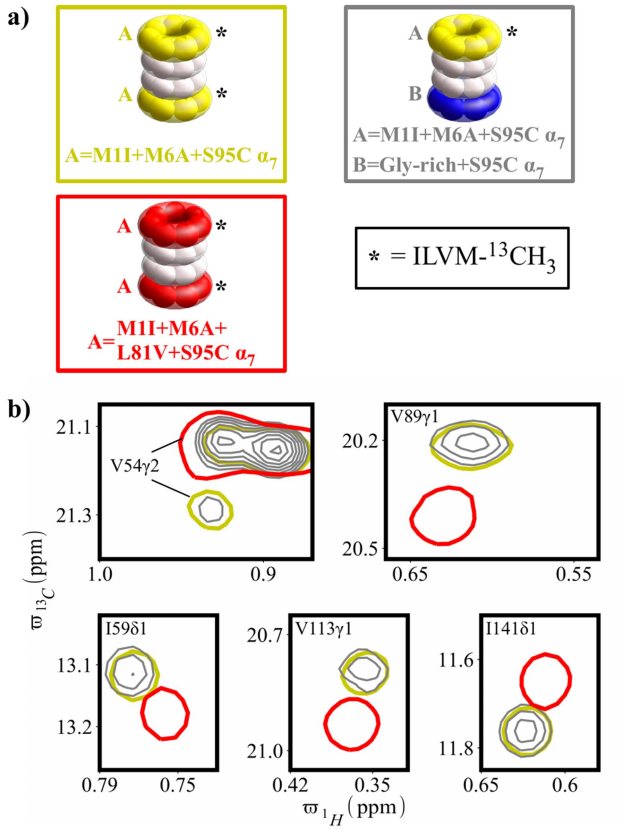

Figure S4. Gly-rich gates at one end of the 20S CP do not trigger the allosteric pathway in the other half of the proteasome. (a) 20S CP molecules used in the study, with the NMR active α_7-rings indicated by an asterisk (*). (b) Regions of ^{13}C-^{1}H HMQC spectra of selected residues showing CSPs upon the L81V mutation. Note that the NMR-inactive α_7-rings comprised of Gly-rich gates have no effect on the position of cross peaks from the NMR-active M1I+M6A+S95C α_7-rings, as the yellow and grey cross-peaks superimpose.

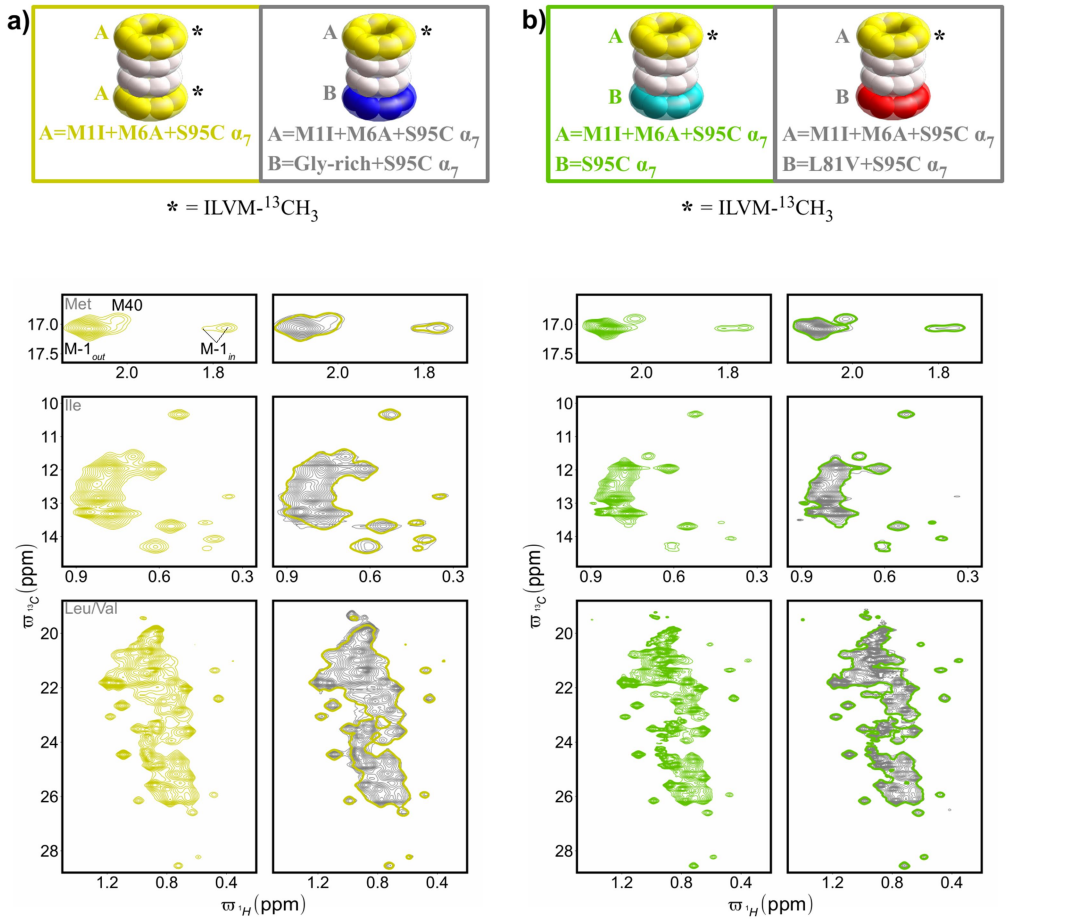

Figure S5. An allosteric path connecting opposite α_7-rings of the 20S CP does not exit. As in Figures 4-5, but including all ^{13}C-^{1}H HMQC spectral regions corresponding to methyl groups from Met, Ile and Leu/Val (top to bottom).

References

1. Religa, T. L.; Sprangers, R.; Kay, L. E., Dynamic regulation of archaeal proteasome gate opening as studied by TROSY NMR. *Science* **2010,** *328* (5974), 98-102.
2. Huang, R.; Perez, F.; Kay, L. E., Probing the cooperativity of Thermoplasma acidophilum proteasome core particle gating by NMR spectroscopy. *Proc Natl Acad Sci U S A* **2017,** *114* (46), E9846-E9854.
3. Delaglio, F.; Grzesiek, S.; Vuister, G. W.; Zhu, G.; Pfeifer, J.; Bax, A., NMRPipe: a multidimensional spectral processing system based on UNIX pipes. *J Biomol NMR* **1995,** *6* (3), 277-93.